




Special Issue Article

Multiple strategies of plant colonization by beneficial endophytic *Enterobacter* sp. SA187

Lukas Synek ^{1,2}, Anamika Rawat,¹
Floriane L'Haridon,³ Laure Weisskopf ³,
Maged M. Saad¹ and Heribert Hirt ^{1,4*}

¹Darwin 21, Center for Desert Agriculture, King Abdullah University of Science and Technology, Thuwal, 23955, Saudi Arabia.

²Institute of Experimental Botany, Czech Academy of Sciences, Rozvojova 263, Prague, 165 02, Czech Republic.

³Department of Biology, University of Fribourg, Fribourg, CH-1700, Switzerland.

⁴Max F. Perutz Laboratories, University of Vienna, Dr. Bohrgasse 9, Vienna, 1030, Austria.

Summary

Although many endophytic plant growth-promoting rhizobacteria have been identified, relatively little is still known about the mechanisms by which they enter plants and promote plant growth. The beneficial endophyte *Enterobacter* sp. SA187 was shown to maintain the productivity of crops in extreme agricultural conditions. Here we present that roots of its natural host (*Indigofera argentea*), alfalfa, tomato, wheat, barley and *Arabidopsis* are all efficiently colonized by SA187. Detailed analysis of the colonization process in *Arabidopsis* showed that colonization already starts during seed germination, where seed-coat mucilage supports SA187 proliferation. The meristematic zone of growing roots attracts SA187, allowing epiphytic colonization in the elongation zone. Unlike primary roots, lateral roots are significantly less epiphytically colonized by SA187. Root endophytic colonization was found to occur by passive entry of SA187 at lateral-root bases. However, SA187 also actively penetrates the root epidermis by enzymatic disruption of plant cell wall material. In contrast to

roots, endophytic colonization of shoots occurs via stomata, whereby SA187 can actively re-open stomata similarly to pathogenic bacteria. In summary, several entry strategies were identified that allow SA187 to establish itself as a beneficial endophyte in several plant species, supporting its use as a plant growth-promoting bacterium in agriculture systems.

Introduction

Similar to the bacterial microflora in the gut of animals, land plants have established beneficial interactions with various bacterial species. During the emergence of land plants, beneficial bacteria most probably helped plants to overcome the challenges brought about by the new stressful environment (Hirt, 2020). Bacterial communities living in tight contact with plants are not only passive consumers (Backer *et al.*, 2018), but play an active role in the promotion of plant growth, development, stress tolerance and resistance to pathogens through various direct or indirect mechanisms (Zamioudis *et al.*, 2013; Peng *et al.*, 2014; Liu *et al.*, 2017; Eida *et al.*, 2019). Therefore, plant growth-promoting rhizobacteria (PGPR) have become an important tool in agriculture as biocontrol agents and biofertilizers, which can significantly improve crop yield (Backer *et al.*, 2018; Saad *et al.*, 2020), due to their ability to help plants to overcome abiotic stresses caused by drought, heat or high salinity (Marasco *et al.*, 2012; de Zélicourt *et al.*, 2013; Tiwari *et al.*, 2017; Cherif-Silini *et al.*, 2019; Mukherjee *et al.*, 2019). These types of stress, representing the most limiting factors that reduce agricultural production (Wang *et al.*, 2003), are currently becoming more severe due to the global climate change.

The vast majority of PGPR have to colonize plant roots to exert beneficial effects. Epiphytic strains colonize root surfaces, whereas endophytic strains occupy also the plant interior (Bisseling *et al.*, 2009; Liu *et al.*, 2017). Many PGPR strains exhibit rather wide host range, making them a versatile tool for agricultural applications (Drogue *et al.*, 2012). Contrary, soil properties and

Received 15 June, 2021; revised 24 August, 2021; accepted 25 August, 2021. *For correspondence. E-mail heribert.hirt@kaust.edu.sa; Tel. (+966) 12 8582959.

climate conditions belong to the most determining factors for establishing beneficial plant–bacterial interactions (Berg and Smalla, 2009). Rhizobacteria are first recruited to the rhizosphere – a critical interface between soil and plant roots where the trade-off between nutrition and defence takes place. They are attracted by root exudates (composed mainly of organic acids, vitamins, simple sugars or polysaccharides) that are actively released by plant roots and influence the physio-chemical properties of the surrounding soil (Bais *et al.*, 2006; Haichar *et al.*, 2014; Massalha *et al.*, 2017b). The polysaccharide-based root mucilage produced by root epidermal cells or root cap cells acts as a lubricant to facilitate root sliding among soil particles and also provides a highly nutritious substrate for occupants of the rhizosphere. Some exudates are found at varying concentrations in different root zones, resulting in distinct patterns of the bacterial colonization along the root (Grayston *et al.*, 1996; Gamalero *et al.*, 2004). Interestingly, depending on stress conditions (Rudrappa *et al.*, 2008; Yuan *et al.*, 2018), plants can shape the microbial community in the rhizosphere by composition of their exudates, and thus control their own colonization (Haichar *et al.*, 2008; Reinhold-Hurek *et al.*, 2015; Massalha *et al.*, 2017b; Ankati and Podile, 2019).

After attraction of PGPR to roots, competent strains can initiate root colonization. Bacterial cells first attach to the root surface non-specifically and reversibly (typically via flagella or pili), and later bind more specifically and irreversibly by production of extracellular polysaccharides or adhesive proteins (Wheatley and Poole, 2018). Subsequently, attached bacterial cells start to proliferate and form colonies that can expand to biofilms, resulting in epiphytic root colonization (Hansen *et al.*, 1997; Rudrappa *et al.*, 2008). PGPR can then use natural openings in the plant body (such as lateral root emergence sites, stomata and hydathodes), root hairs, damaged trichomes or wounds (caused by herbivores, insects, nematodes) as gateways to enter the internal plant tissues (Hardoim *et al.*, 2015). Furthermore, many PGPR produce cell wall-degrading enzymes – especially cellulases, xylanases, pectinases and endo/exo-glucanases – that loosen plant cell-to-cell adhesion in epidermis and enable active entry of bacteria into root tissues (Quadt-Hallmann *et al.*, 1997; Compant *et al.*, 2005; Reinhold-Hurek *et al.*, 2006; Sessitsch *et al.*, 2012). Some PGPR can even cross the endodermis and colonize the entire plant body via plant vessels (Frank *et al.*, 2017).

Since efficient colonization is supposed to be a critical factor for plant growth promotion by rhizobacteria we performed a comprehensive microscopic analysis of plant colonization by *Enterobacter* sp. SA187. This bacterial strain was originally isolated as a root endophyte from *Indigofera argentea*, a leguminous plant occupying semi-

desert areas in the Arabian Peninsula (Andres-Barrao *et al.*, 2017), and was revealed to efficiently induce multi-stress tolerance in *Arabidopsis*, alfalfa and wheat (de Zélécourt *et al.*, 2018). In this report, we describe that SA187 is attracted to hydrated seed coats, accumulates in the region of future root emergence, and then immediately colonizes young roots in *Arabidopsis*. Later, SA187 preferentially colonizes primary roots over lateral roots. Due to production of pectinases and proteolyases SA187 can actively penetrate the root epidermis besides its passive entry at lateral root bases to colonize the root interior. SA187 also enters shoot tissues through stomata that can be actively opened by SA187 after their initial closure. SA187 rapidly colonizes seedlings of its native host both epiphytically and endophytically with an interesting accumulation in secretory trichomes. SA187 could also colonize seedlings of four crop plants, especially wheat and barley that showed remarkably fast endophytic colonization.

Results

Rapid epiphytic and endophytic colonization of the native host by SA187

Enterobacter sp. SA187 was originally isolated as a root endophyte from *I. argentea* (Fig. 1A) (Andres-Barrao *et al.*, 2017). Therefore, we first inspected colonization of 2- to 7-day-old *Indigofera* seedlings grown in pots with sterile sandy soil inoculated by GFP-tagged SA187.

The root surface was epiphytically colonized by SA187 forming colonies of various sizes (Fig. 1B). Many motile SA187 cells were detected in the intercellular space of root tissues as early as 2 days after germination (Fig. 1C and D) that later established colonies in the root cortex (Fig. 1E). Hypocotyls were also efficiently colonized both epiphytically and endophytically, generating long linear colonies between epidermal cells and cortical cells, respectively (Fig. 1F and G).

Contrary to roots and hypocotyls, we found no extensive colonization of the surface and interior of cotyledons and young primary leaves, except for putative secretory trichomes (Fig. 1H). While no SA187 colonization of the predominant hairy trichomes was observed (Fig. 1H), the lumen of short oval trichomes was entirely filled with SA187 cells (Fig. 1I). Microscopic inspection of these internally colonized trichomes revealed that they were intact rather than damaged.

Since glandular secretory trichomes are known as sites of volatile production, which plays an important role in defence against herbivores and pests (Glas *et al.*, 2012), we investigated whether colonizing bacteria (SA187) could be responsible for the production of volatiles. Indeed, the analysis by gas chromatography–mass

spectroscopy (GC-MS) detected a number of volatiles released by SA187, including a significant amount of indole (representing 88% of the total chromatogram area), various pyrazines, 2-phenylethanol and three

different sulphur-containing volatiles detected at lower levels but with high confidence (Table S1; Fig. S1). Genome analysis confirmed that SA187 possesses genes encoding tryptophanase (*tnaA*) for the tryptophan

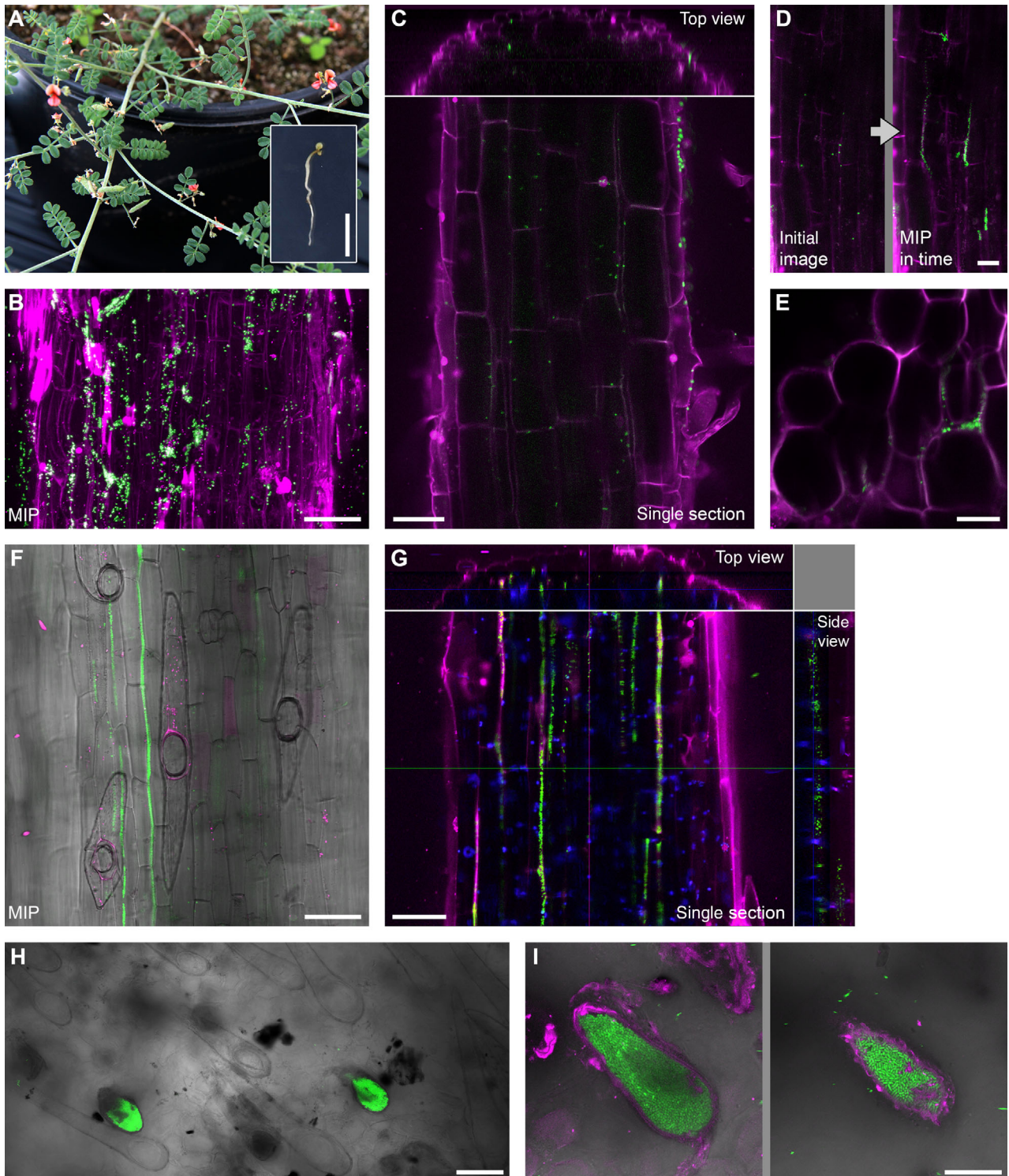


Fig. 1. Legend on next page.

conversion to indole and an efflux pump (*acrEF*) for indole excretion (Kawamura-Sato *et al.*, 1999; Li and Young, 2013).

Taken together, isolated SA187 can efficiently colonize roots, hypocotyls and secretory trichomes of its native host, *I. argentea*, in experimental conditions.

Several crop plants can be colonized by SA187

Field experiments with both monocot and dicot crops showed that SA187 can enhance the performance of crops in desert agriculture (de Zélicourt *et al.*, 2018; Shekhawat *et al.*, 2021). We therefore focused on root colonization of alfalfa, tomato, wheat, and barley seedlings. Microscopic analysis revealed that their roots exhibited extensive epiphytic colonization similarly to *Indigofera* under the experimental conditions (Fig. 2).

The endophytic root colonization by SA187 was absent in tomato, sparse with single SA187 cells in alfalfa, but very common in the case of wheat and barley seedlings when evaluated 3 and 7 days after *in vitro* germination (Fig. 2). Moreover, in wheat and barley, SA187 formed colonies inside the root tissues as early as 3 days after germination. These differences in the root penetration suggest a certain degree of SA187 host specificity for endophytic root colonization.

Seed coat colonization precedes root colonization in *Arabidopsis*

Previously, we showed that SA187 could act as a beneficial endophyte in *Arabidopsis thaliana* and colonized its seedlings (de Zélicourt *et al.*, 2018). We therefore employed *Arabidopsis* as a model plant to study the plant colonization in detail, starting with the process of seed germination.

Within 1 day upon placement of dry *Arabidopsis* seeds on SA187-inoculated agar plates, SA187 efficiently proliferated in the seed-coat mucilage and started to colonize seed surfaces (Fig. 3A). Remarkably, large SA187

colonies preferentially developed at the micropylar seed pole rather than on the opposite pole or central regions of the surface in pre-germinating seeds (Fig. 3A, F and G; Fig. S2). At the micropylar seed pole, the seed coat later ruptures to allow for radicle emergence. Two days post inoculation, during the very beginning of seed germination, SA187 accumulated in the seed-coat rupture (Fig. 3B and C). Emerging radicles developing into roots were immediately colonized by SA187, representing the initiation of root colonization (Fig. 3D and E).

Epiphytic colonization of *Arabidopsis* roots by SA187 is initiated in actively growing root tips

For detailed description of root colonization by SA187, we investigated whether the SA187 attraction to roots and the initiation of colonization is dependent on a specific morphological root zone.

In liquid medium, mobile SA187 cells were attracted to root tips with maximal accumulation in the meristematic and early elongation zones (Fig. 4A). On vertical agar medium, however, inoculated roots were surrounded by a distinct translucent layer, where SA187 reached high cell numbers, indicative of stimulated bacterial proliferation, along the entire root (Fig. 4B). Due to the high density of SA187 cells, we were unable to determine whether SA187 is attracted to a specific root zone. Sterile seedlings had no translucent layer around their roots, indicating that this layer was only produced upon SA187-plant interaction (Fig. S3).

Focusing on the competence for epiphytic colonization by SA187, 4-day-old seedlings were transferred from sterile agar plates to SA187-containing agar plates and cultivated under the same conditions (see Fig. S4 for details of the experimental setup). Using confocal microscopy (1 day after the transfer) and cultivation-based quantification (2 days after the transfer), we found that only those root regions were stably colonized that developed after seedling transfer, whereas old root regions (already present before transfer) were sparsely colonized

Fig. 1. Colonization of *Indigofera* seedlings in sterile sandy soil by GFP-tagged SA187.

A. *Indigofera argentea* – potted mature 2-month-old plant. Inset shows 3-day-old seedling. Scale bar = 1 cm.

B. Epiphytic colonization of primary root. Scale bar = 50 μ m.

C. Endophytic colonization of the root interior. Selected image of a Z-stack and orthogonal top view. Scale bar = 50 μ m.

D. Bacterial cells move freely in the intercellular space: Initial image and MIP of a time-lapse series are displayed (8 min by 10 s). Scale bar = 50 μ m.

E. Detail of bacterial colony in the intercellular space at the root-shoot junction. Scale bar = 25 μ m.

F. Epiphytic hypocotyl colonization of seedling grown in high air humidity in a closed jar (merged fluorescence and DIC image). Scale bar = 50 μ m.

G. Endophytic hypocotyl colonization of seedling grown in soil in low air humidity in the greenhouse. Selected confocal section from a Z-stack with a top and side orthogonal views. Scale bar = 50 μ m.

H. Colonization of secretory trichomes on the upper cotyledon leaf epidermis. Scale bar = 50 μ m.

I. Two optical sections of the same secretory trichome filled with bacterial cells. Scale bar = 25 μ m.

Green – GFP-tagged SA187; magenta – cell walls stained by PI, which also stains dead bacterial cells; blue – chlorophyll autofluorescence; grey – DIC; MIP, Maximum Intensity Projection.

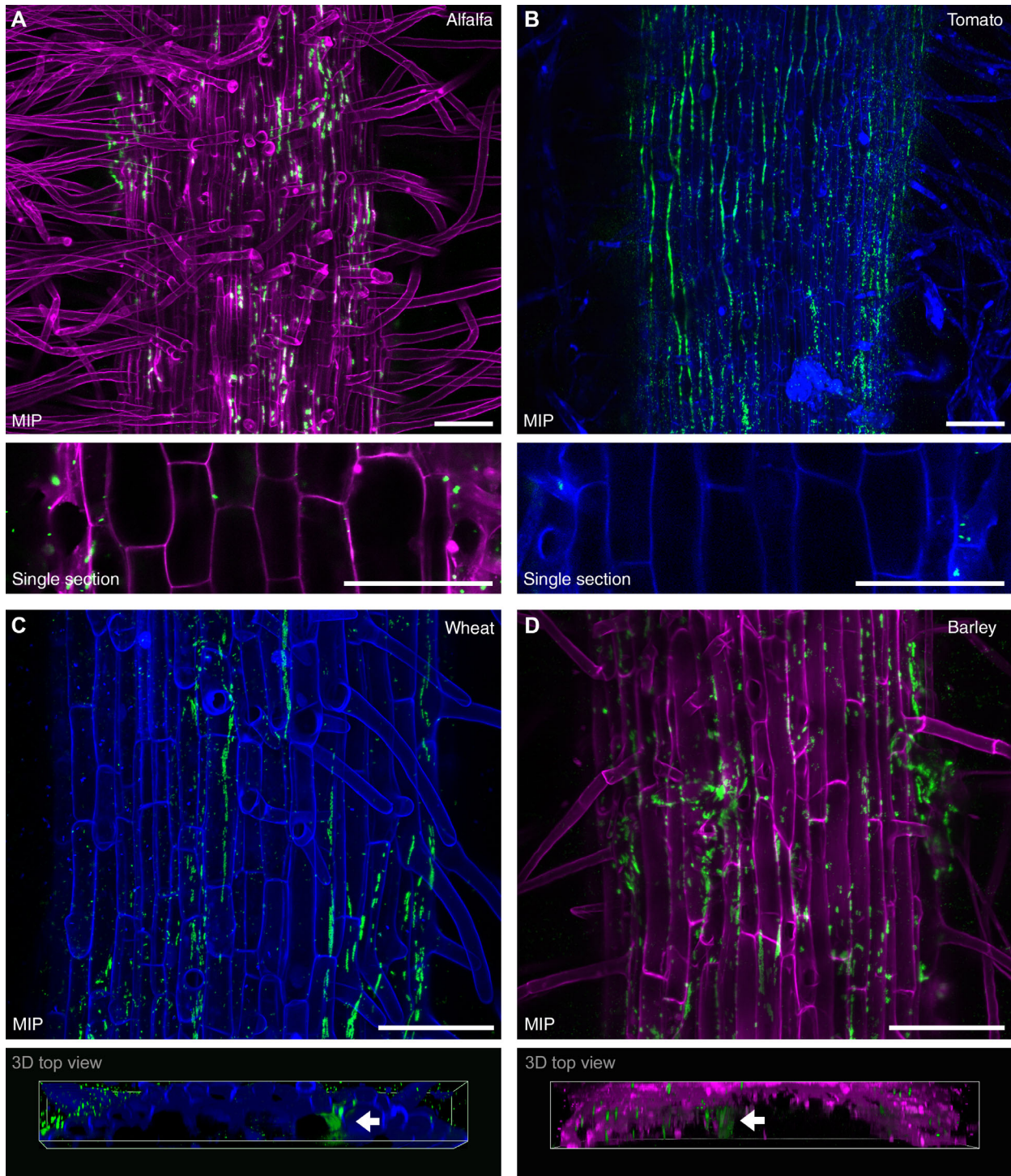


Fig. 2. Colonization of alfalfa, tomato, wheat, and barley roots by GFP-tagged SA187 *in vitro*.

A. Epiphytic and endophytic root colonization in 3-day-old alfalfa seedling. Lower panel shows SA187 cells in the intercellular space of root cortex.

B. Epiphytic root colonization in 3-day-old tomato seedling.

C. Epiphytic and endophytic root colonization in 3-day-old wheat seedling. Lower panel displays a large colony (marked by arrow) inside the root cortex in a 3D reconstruction.

D. Epiphytic and endophytic root colonization in 3-day-old barley seedling. Lower panel displays a large colony (marked by arrow) inside the root cortex in a 3D reconstruction.

Representative images from observation of at least 30 seedlings in three biological replicates. Green – GFP-tagged SA187; magenta or blue – cell walls stained by PI. Scale bars = 100 μm .

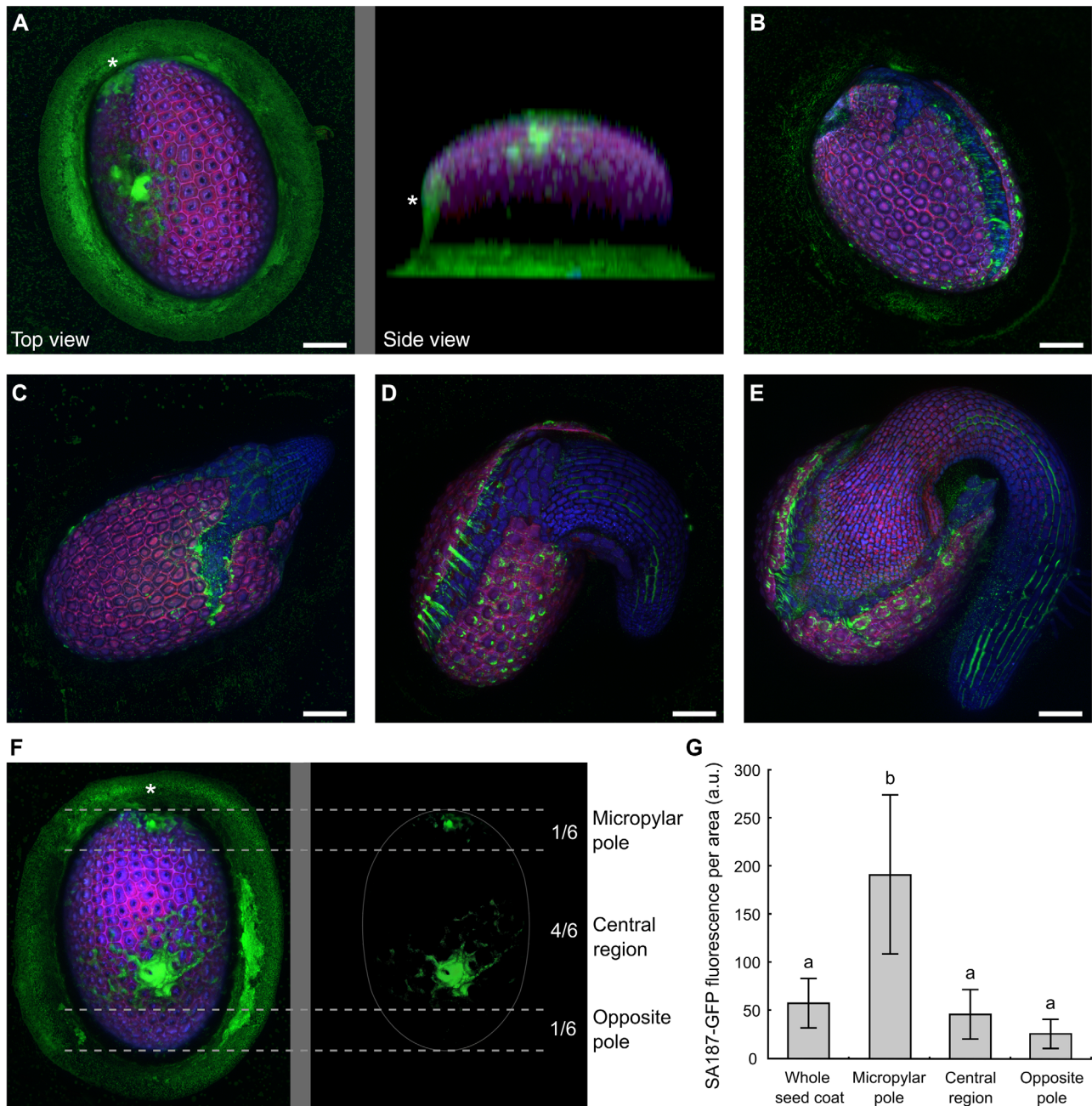


Fig. 3. Arabidopsis seeds and nascent seedlings colonized by GFP-tagged SA187 in 3D reconstructions.

A. Seed colonization 1 day post inoculation (DPI) by plating on $\frac{1}{2}$ MS agar plates containing SA187. SA187 propagates in the hydrated seed-coat mucilage and colonizes typically the micropylar region (marked by asterisk) and occasionally random sites of the seed coat.

B, C. Bacterial cells accumulate in the seed coat rupture (2 DPI).

D, E. Colonization of an emerging radicle (2–3 DPI). SA187 shows clear preference towards the radicle rather than to cotyledons.

F. Schematic display of SA187-GFP fluorescence measurement in different seed coat regions. Polar regions were defined here as one sixth of the seed length.

G. Quantification of SA187-GFP fluorescence in different seed coat regions. Mean \pm SD is shown, $n = 39$ seeds. Letters denote statistically different groups as evaluated by ANOVA at the 0.01 significance level.

Panels A to E are representative images from observations of more than 60 germinating seeds in three biological replicates. Green – GFP-tagged SA187; magenta – red autofluorescence; blue – far-red autofluorescence. Except for (A), lower parts of seeds and the agar surface were excluded from confocal Z-stacks for clarity. All scale bars = 100 μ m.

by SA187 (Fig. 4C and D). This observation suggests that SA187 colonization could be efficiently initiated only in actively growing root tips. To test whether this is due to

anatomical features or growth activity of roots, shoots were removed and the shoot-less roots were transferred to SA187-containing agar plates (Fig. S4). Those roots

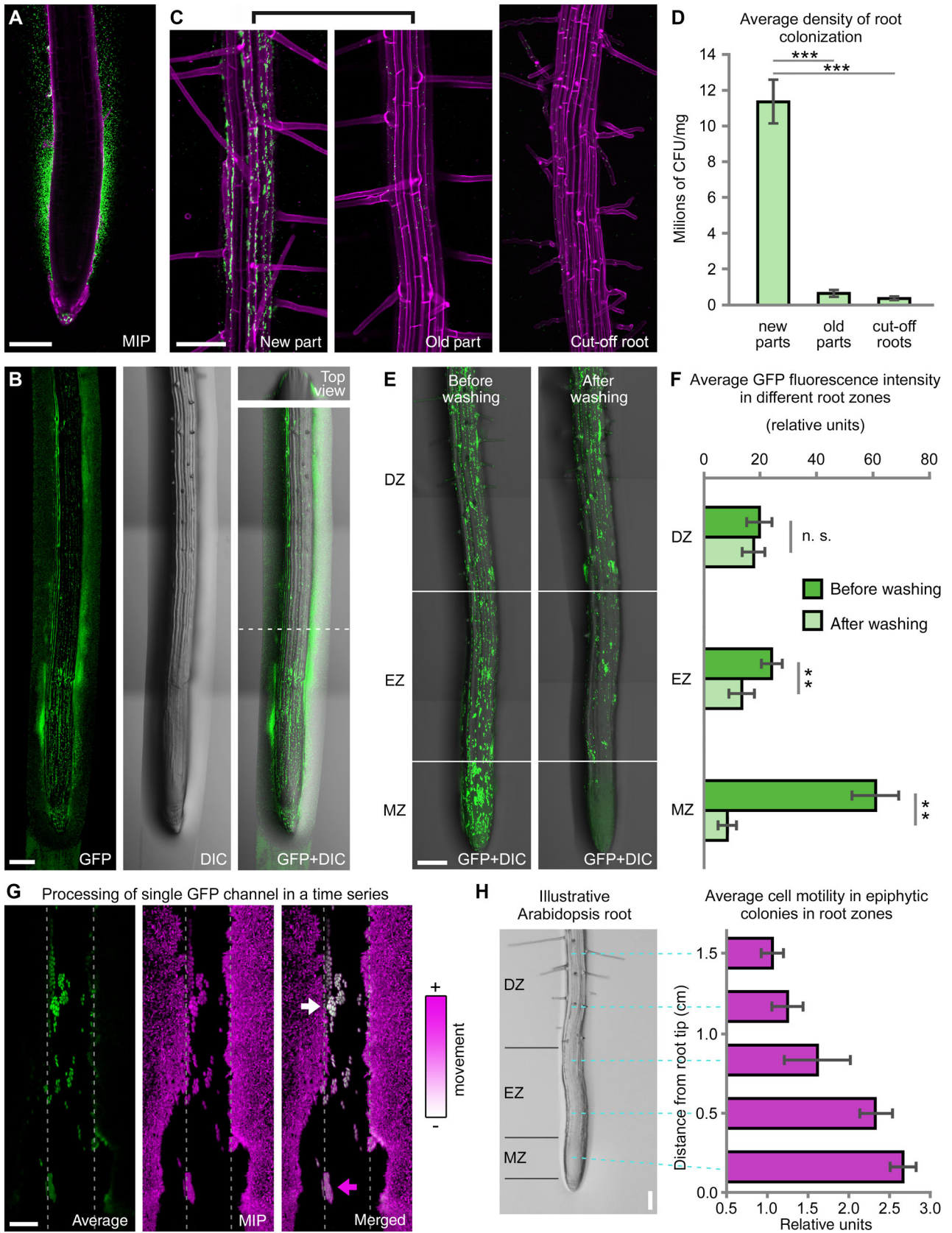


Fig. 4. Legend on next page.

soon stopped growth and showed minimal colonization in contrast to intact seedlings (Fig. 4C and D), indicating that anatomical features of root tips are not sufficient for efficient colonization by SA187.

To determine the degree of stable bacterial attachment to different developmental zones, SA187-colonized roots were imaged before and after gentle washing (Fig. 4E). Quantification based on SA187-GFP fluorescence showed that bacterial cells were highly attracted to the meristematic zone, but their attachment was rather weak in this zone, in contrast to the increasingly tight attachment observed in the elongation and differentiation zones (Fig. 4F).

Motility of SA187 on root surfaces was analysed in different root zones (without root washing prior to imaging). Analysis of captured time-lapse images showed that SA187 cells gradually lost their motility upon attachment to root surfaces (Fig. 4G and H). In the meristematic zone, SA187 cells were often attached by one end and still vibrated around attachment points. In the elongation zone, and later in the differentiation zone, most SA187 cells exhibited no motility, leading to stable epiphytic root colonization.

Lateral roots allow for passive entry of SA187, but are less colonized than primary roots in Arabidopsis

We previously observed that stably attached SA187 cells first produced small colonies – typically in grooves between epidermal cells – that later developed into discontinuous biofilms on the root epidermis (de Zélicourt *et al.*, 2018). In the current study, we observed that lateral roots were significantly less colonized than primary

roots and these differences persisted for at least 3 weeks after germination (Fig. 5A). This observation was verified by cultivation-based quantification of the extent of SA187 colonization on apical root parts harvested from primary and lateral roots of 16-day-old plants (Fig. 5B).

Since SA187 is a root endophyte that can occupy the intercellular space of Arabidopsis root tissues (de Zélicourt *et al.*, 2018), we aimed to study its modes of entry in detail. Large SA187 colonies were often found at the lateral root emergence site, both above and below the epidermis, even before the nascent lateral root broke through the epidermis (Fig. 5C). When sterile seedlings were placed into liquid medium with SA187, bacterial cells were equally attracted to emerging lateral roots as to wounds (caused by mechanical damage) at 30 min after contact (Fig. 5D and E). Openings around lateral root emergence sites then allowed SA187 to enter the root interior (Fig. 5F), representing an important gateway for passive bacterial entry. In cavities around lateral root bases, SA187 established colonies and started endophytic colonization of the intercellular space in primary root tissues (Fig. 5G). Prominent epiphytic colonization often developed around lateral root emergence sites in the case of established and elongating lateral roots (86%; $n = 56$) (Fig. 5H).

SA187 can actively cross the root epidermis to colonize roots endophytically

Next, we addressed the possibility that SA187 can actively penetrate root tissues in Arabidopsis. To eliminate passive entry at sites of lateral root emergence or damaged epidermal cells, only root regions between first lateral roots and the root tip were examined and samples

Fig. 4. Progress of Arabidopsis root colonization by GFP-tagged SA187.

A. SA187 in liquid medium shows the highest attraction to meristematic and early elongation root zones. MIP of a time-lapse series (5 min by 10 s). Representative image from 25 similar observations. Green – GFP-tagged SA187; magenta – cell walls stained by PI. Scale bar = 100 μm .
 B. Translucent layer surrounding colonized roots on agar surface. MIP of a Z-stack assembled from 3 tiles. In the inset, top view of an orthogonal projection generated at the position indicated by the dashed line. Representative image from the analysis of 30 seedlings in three biological replicates. Green – GFP-tagged SA187; grey – DIC. Scale bar = 100 μm .
 C. Intact and shoot-less 4-day-old seedlings were transferred from sterile to SA187-inoculated agar plates for 1 day. Root colonization was imaged in parts already present before transfer (old part), and in newly grown part (new part). Cut-off roots were imaged at the same distance from root tips as for the new parts. See Fig. S4 for the experimental setup. Representative image from the analysis of 45 seedlings in three biological replicates. MIP of confocal Z-stacks; green – GFP-tagged SA187; magenta – cell walls stained by PI. Scale bar = 100 μm .
 D. Cultivation-based quantification of root colonization in (C). Bars represent mean \pm SD, $n = 36$. Bars represent mean \pm SD. Asterisks indicate statistically different pairs (t -test; $P < 0.001$).
 E. SA187 attachment to different root zones of the same root before and after washing. Representative image from the analysis of 21 seedlings in three biological replicates. MIP of a confocal Z-stack; GFP-tagged SA187 fluorescence (green) combined with DIC (grey). MZ, meristematic zone; EZ, elongation zone; DZ, differentiation zone. Scale bar = 100 μm .
 F. Fluorescence-based quantification of root colonization in different root zones of 21 roots in (E). Bars represent mean \pm SD, $n = 63$ for DZ and EZ, $n = 21$ for MZ. Asterisks indicate statistically different pairs (t -test; $P < 0.01$).
 G. Representative image documenting the visualization of cell motility. Average projection and maximum intensity projection (MIP) of SA187-GFP fluorescence generated from a time series (3 min by 2 s). In the merged image, white colour indicates no movement, while magenta an intensive movement. Examples of colonies with motile cells (magenta) and non-motile cells (white) are marked by arrows. Root surface in focus (aligning to cover glass) is bordered by dashed lines. Scale bar = 10 μm .
 H. Quantification of cell motility within SA187 colonies in different root zones. MZ, meristematic zone; EZ, elongation zone; DZ, differentiation zone. The motility was assessed on 18 roots from three biological replicates. Bars represent mean \pm SD, $n > 95$. Scale bar = 100 μm .

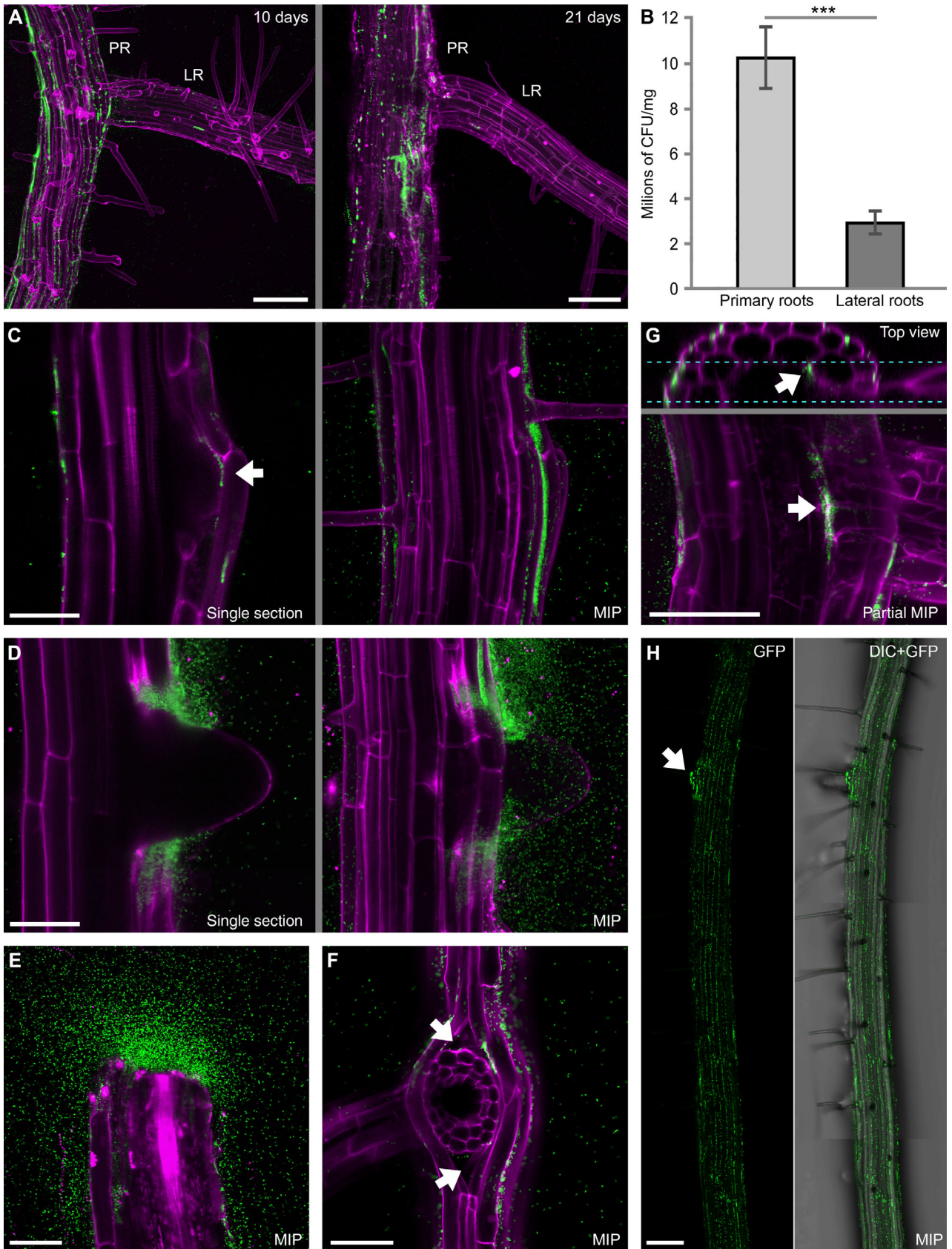


Fig. 5. Legend on next page.

were stained with propidium iodide (PI, to uncover damaged cells), respectively.

GFP-tagged SA187 single cells or small colonies were detected in the intercellular space of the cortex of intact apical root parts, but not earlier than 7 days after germination, suggesting an active, yet slow, mechanism of SA187 entry into roots (Fig. 6A). The internalized GFP-tagged SA187 cells were consistently found in the differentiation zone, while meristematic and elongation zones remained free of internalized bacteria. We also never observed SA187 inside intact plant cells.

In addition, we used *slr-1* seedlings deficient in lateral root production (Fukaki *et al.*, 2002). GFP-tagged SA187 was detected in 12-day-old roots of *slr-1* seedlings with similar occurrence as in wild-type seedlings (*slr-1*: 3.3 ± 1.6 cases per cm; WT: 2.4 ± 1.5 cases per cm; $n = 18$; Student's *t*-test $P = 0.091$), suggesting that SA187 uses an active entry mechanism to penetrate roots that is independent of lateral root emergence (Fig. S5).

To assess whether SA187 might produce specific enzymes to degrade components of the plant cell wall, the SA187 genome was analysed (Andres-Barrao *et al.*, 2017). No homologues to genes encoding cellulases were identified, but multiple genes encoding putative pectinases were found, which can digest pectins via the catabolism of hexuronate D-galacturonate in the isomerase pathway (Table S1). In parallel, enzymatic assays for cellulase, pectinase and protease activity, respectively, revealed that SA187 possesses no cellulase, but moderate pectinase and protease activities, indicating the potential of SA187 to enzymatically degrade plant cell wall components – most likely the pectin-based middle lamella (Fig. 6B). This observation explains the capacity of SA187 to penetrate the root epidermis and enter the intercellular space of roots.

SA187 can actively re-open stomata for endophytic shoot colonization

Imaging by confocal microscopy showed that cotyledons, petioles and hypocotyls of Arabidopsis seedlings were

epiphytically colonized by SA187 in grooves between epidermal cells and also endophytically in intercellular spaces (Fig. 7). SA187 cells were directly observed entering these organs via stomata (Fig. 7D–G). Microscopic inspection of 2-week-old *speechless* mutants, that completely lack stomata, revealed no SA187 cells in the interior of shoots, confirming that stomata are the gateway for SA187 entry into above-ground organs (Fig. 7E). Indeed, SA187 was also regularly observed in both open and closed stomata, suggesting an active attraction to these pores (Fig. 7F–G; Fig. S6).

To test if SA187 can overcome stomatal immunity, and re-open stomata after initial closing by detection of microbe-associated molecular patterns (MAMPs), we treated Arabidopsis leaf segments with SA187 and then measured stomatal aperture after 1 and 3 h. In parallel, we used *P. syringae* DC3000 (*Pst*) as a positive control and abscisic acid (ABA) as a negative control for stomatal re-opening. Upon contact with Arabidopsis leaves, *Pst* triggers stomatal closure within 1 h, but reverts the process at 3 h due to production of coronatine (Melotto *et al.*, 2006). The incubation with SA187 or *Pst* led to efficient stomatal closure after 1 h, indicating that MAMPs of SA187 are equally detected by Arabidopsis. However, in contrast to ABA, partial re-opening of stomata was observed in samples treated with *Pst* or SA187 after 3 h (Fig. 8). Although no genes encoding the conventional coronatine biosynthesis were found in the SA187 genome, these results indicate that, similar to *Pst*, SA187 uses an active stomatal re-opening mechanism for entry into Arabidopsis leaf tissues.

Discussion

Although many endophytic PGPR strains have been identified by now, relatively little is still known about the mechanisms by which these bacteria enter plants and promote plant growth. We observed similar colonization on roots of several plant species, including crops, which is in agreement with our previous findings that SA187

Fig. 5. Colonization of primary and lateral roots and passive entry of SA187 into roots in Arabidopsis seedlings.

A. MIP of confocal Z-stacks taken in upper parts of root systems. Scale bars = 100 μ m.

B. Quantification of colonization using cultivation-based counting. In total, 12 samples for each root type were evaluated in three biological replicates. Bars represent mean \pm SD, $n = 36$, *t*-test $P < 0.001$, asterisks indicate a high statistical significance.

C. SA187 colonies at the tip of a nascent lateral root below epidermis (marked by arrow) and at the epidermal surface above the emergence site before lateral root outgrowth in 7-day-old colonized seedlings. MIP of a Z-stack. Scale bar = 50 μ m.

D. Attraction of SA187 to young emerged lateral root at 30 min after contact with a sterile seedling. MIP of a Z-stack. Scale bar = 50 μ m.

E. Attraction of SA187 to a wound site at 30 min after contact with a sterile separated primary root. MIP of a time-lapse series (2 min by 5 s). Scale bar = 50 μ m.

F. SA187 cells entering a cavity at a lateral root base via openings (marked by arrows) in the case of a 7-day-old colonized seedling. MIP of a Z-stack. Scale bar = 50 μ m.

G. Large SA187 colony (marked by arrows) at the base of a lateral root of a 10-day-old colonized seedling. Top view of an orthogonal projection and a partial MIP of a Z-stack (sections between dashed lines). Scale bar = 50 μ m.

H. Enhanced epiphytic colonization around a lateral root emergence site (marked by arrow) in a 7-day-old colonized seedling. Scale bar = 100 μ m.

All panels (except for B) show representative images from the analysis of at least 60 seedlings (A) or 30 similar observations (C–H) from three independent experiments. Green – GFP-tagged SA187; magenta – cell walls stained by PI; grey – DIC.

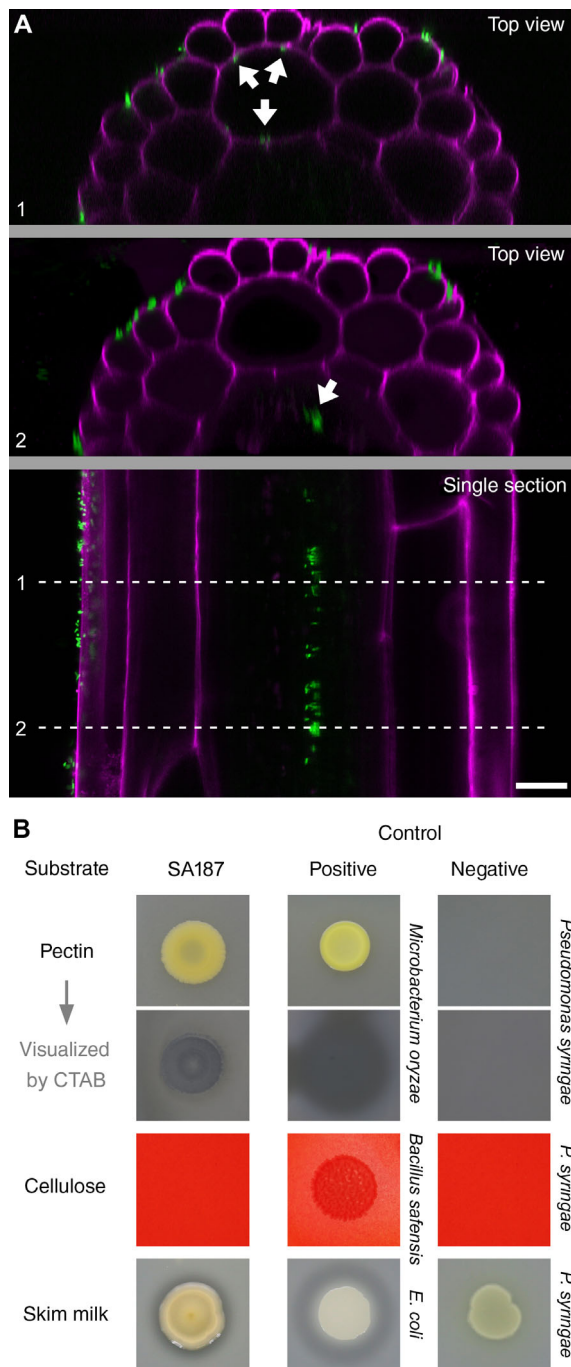


Fig. 6. Active entry of SA187 into Arabidopsis roots.

A. Internalized GFP-tagged SA187 in the apoplast of the differentiation root zone below the region of lateral root formation. Selected section from a Z-stack and two orthogonal projection at indicated positions (1, 2). Bottom projection shows that SA187 can cross the endodermis. Representative images from the analysis of at least 50 roots from three independent experiments. Scale bar = 10 μm .

B. The growth medium was composed only of agar and either pectin, cellulose or skim milk. Enzymatic activity is indicated by clear zone around a bacterial colony. Pectin degradation was evaluated after washing colonies off and staining with CTAB detergent. Representative results from one of three independent experiments; each combination was plated in six technical replicates.

can maintain the productivity of crops in extreme agriculture and is hence a PGPR for both monocot and dicot species (de Zélicourt *et al.*, 2018; Shekhawat *et al.*, 2021). Since efficient plant colonization is a critical factor for the action of PGPR, we characterized here the plant colonization by *Enterobacter* sp. SA187 focusing on its interaction with the model plant *A. thaliana*. Colonization experiments in native soil, i.e. in the presence of natural microbial community, would be an interesting future extension to our simplistic experimental setup with the isolated SA187 strain.

In natural conditions, plants come into contact with PGPR as seeds in the soil. Presence of the seed coat mucilage, termed the myxospermy, is a common feature of most angiosperm plants. This hydrophilic gel-like mucilage is generated by instant hydration of pectins deposited in epidermal cells of the seed coat. The strong colonization of hydrated Arabidopsis seed coats by SA187 shows that the highly nutritious seed-coat mucilage supports the proliferation of beneficial bacteria to prepare an inoculum, which might be an important factor for subsequent root colonization under natural conditions. We hypothesize that the preferential accumulation of SA187 at the micropylar region prior to germination might be due to the release of attracting compounds through the semi-permeable seed coat (De Giorgi *et al.*, 2015). Such attractants might originate in the micropylar endosperm that surrounds the radicle and contains storage sugars (Morley-Smith *et al.*, 2008). Therefore, the seed-coat mucilage might have an additional important function in plant colonization by PGPR besides the promotion of seed hydration, prevention of gas exchange and attachment to soil substrates or animal vectors (Haughn and Western, 2012).

The active exchange of signalling molecules and metabolites between bacteria and plant roots is essential to establish beneficial interactions (Haichar *et al.*, 2014). Our experiments in Arabidopsis showed that normal root growth and secretory activity, which depend on a functional shoot–root system, are crucial for the initiation of root colonization by SA187, while physical and chemical properties of root surfaces are not sufficient for this process. Especially the outer domain of epidermal cells in the meristematic zone, defining the root-soil interface and characterized by intensive secretion (Langowski *et al.*, 2010; Fendrych *et al.*, 2013), represents a critical element to establish root colonization. Flavonoids and malic acid were documented to enhance particular steps in root colonization by several bacterial species (Webster *et al.*, 1998; Balachandar *et al.*, 2006; Rudrappa *et al.*, 2008), but what compounds secreted from roots are required for SA187 colonization remains to be investigated. High production of root mucilage in the meristematic zone and root cap supports SA187 proliferation,

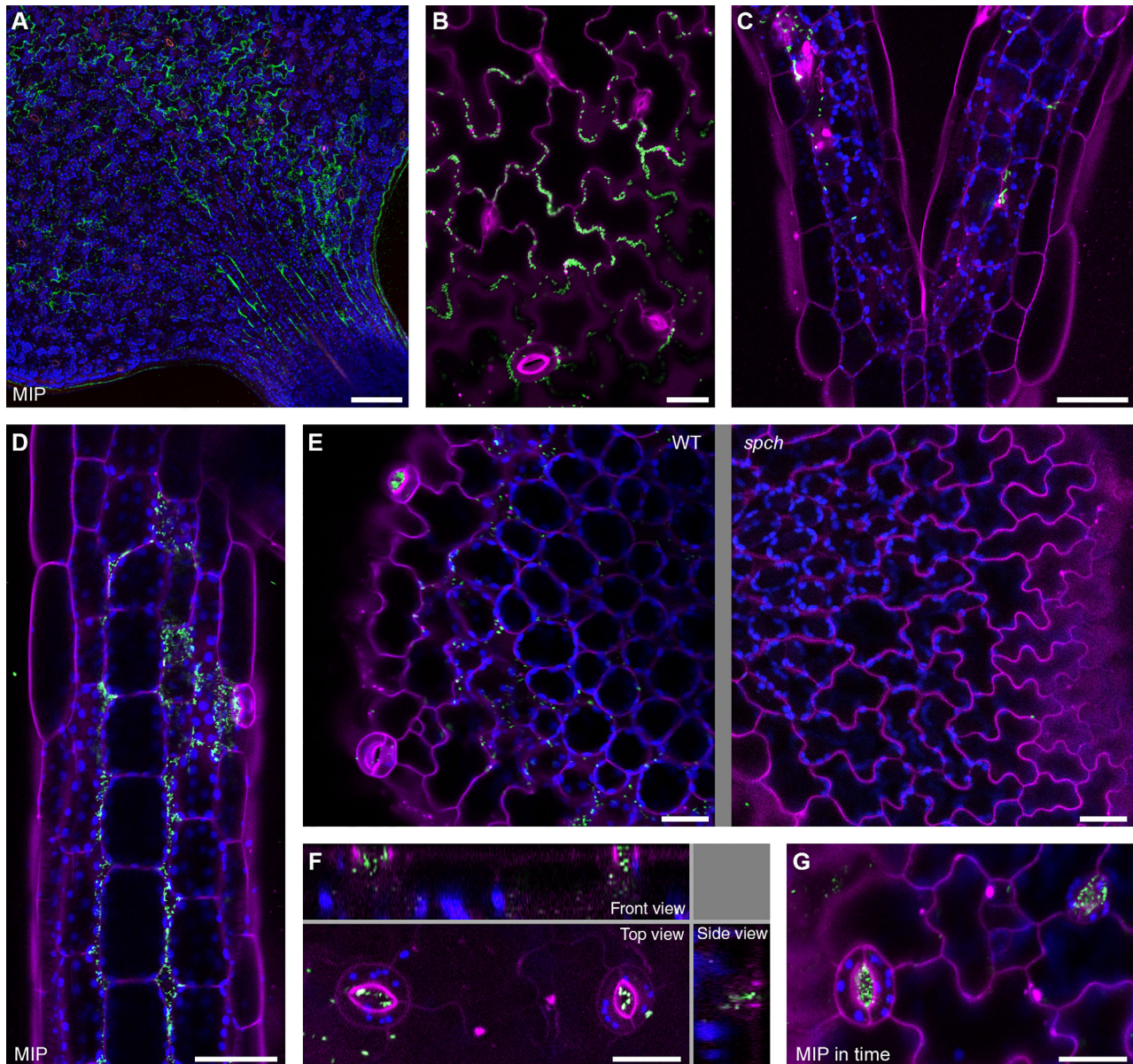


Fig. 7. SA187 enters into Arabidopsis shoots via stomata.

A. Epiphytic cotyledon colonization in a 7-day-old seedling. Scale bar = 100 μ m.

B. Colonized cotyledon in detail. SA187 typically colonizes grooves between epidermal cells. Scale bar = 20 μ m.

C. Endophytic colonization of petioles in 7-day-old seedling. Scale bar = 50 μ m.

D. Endophytic colonization of a hypocotyl. SA187 cells accumulate at a stoma. Scale bar = 50 μ m.

E. Endophytic colonization normally occurs in wild-type but not in *speechless* mutant cotyledons. Due to the concave shape of cotyledons, centres of both optical sections depict the mesophyll (marked by presence of chloroplasts), while peripheries show the epidermal surface. Scale bar = 20 μ m.

F. SA187 entry through stomata in cotyledons. Note that moving bacterial cells could be captured multiple times during the Z-stack imaging (35 s). Scale bar = 20 μ m.

G. MIP generated from a time-lapse series (2 min by 5 s) showing attraction of SA187 to stomata in cotyledons. Scale bar = 20 μ m.

All panels are representative images from the analysis of at least 30 seedlings from at least three independent experiments. Green – GFP-tagged SA187; magenta – cell walls stained by PI; blue – chlorophyll autofluorescence.

but most likely mechanically prevents bacterial attachment to the root surface at the same time. This might simply explain that while SA187 was attracted to the meristematic root zone, the onset of stable colonization

occurred in the elongation zone, as shown also for *Pseudomonas fluorescens* SBW25 on maize roots (Humphris *et al.*, 2005). Not necessarily exclusive, heterogeneous root zone secretion of certain exudates may explain this

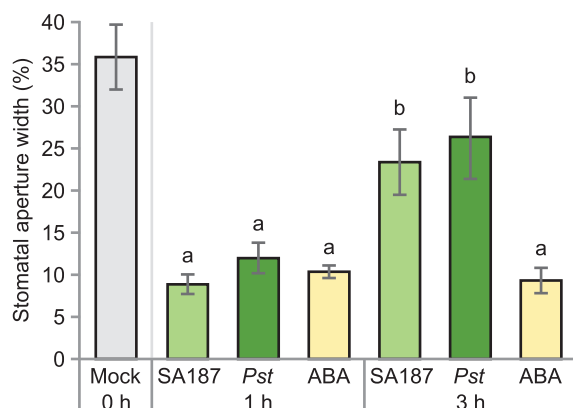


Fig. 8. SA187 can re-open stomata in *Arabidopsis* leaves. Leaf segments treated *in vitro* with SA187, *Pst* (*Pseudomonas syringae* pv. *tomato* DC3000) or abscisic acid (ABA). Mean widths of stomatal apertures are displayed after normalization to untreated samples at the start of the experiment (at least 30 stomata measured per leaf segment). The experiment was done on three leaf segments per condition in three biological replicates ($n = 9$), error bars are SD; letters denote statistically different groups as evaluated by ANOVA at the 0.01 significance level.

topological specificity as observed for several root colonizing bacteria (Hurek *et al.*, 1994; Gamalero *et al.*, 2004; Massalha *et al.*, 2017a). The resulting root colonization pattern generated by SA187 at the microscopic scale resembles that of several characterized PGPR, suggesting the colonization pattern might be dictated by the nutrient regime or/and interactions between the host and PGPR (Hansen *et al.*, 1997; Rudrappa *et al.*, 2008; Massalha *et al.*, 2017a).

Interestingly, we found that lateral roots were dramatically less colonized than primary roots in *Arabidopsis*. A single publication (Dietel *et al.*, 2013) documented a similar observation that *Bacillus amyloliquefaciens* FZB42a bearing a mutation in *pabB* (involved in biofilm formation) exhibited compromised colonization of young lateral roots in contrast to primary roots. These findings suggest that principal physiological differences exist between primary and lateral roots, which are critical for the initiation of bacterial colonization and might again reside in specific secretion patterns.

Endophytes can passively enter the plant root tissues through lateral root emergence sites or wounds. In fact, since lateral roots are initiated in the pericycle and have to mechanically penetrate three tissue layers during their development, the emergence sites can be considered equivalent to wounds and as such they release chemical compounds attracting PGPR (Stoeckle *et al.*, 2018). Moreover, like many other PGPR, SA187 is endowed by an active penetration mechanism using enzymatic degradation of plant cell walls. The pectinase and protease activity of SA187 indicates its potential to digest the

middle lamella – an extracellular layer above the primary cell wall that cements plant cells together and is composed primarily of pectins (Zamil and Geitmann, 2017). Thus, SA187 can weaken cell-to-cell adhesion of root epidermal cells and open a gateway to the intercellular space in root tissues even without digesting cellulose fibres.

Although isolated SA187 uses a similar mechanism of epiphytic root colonization in diverse plant species, endophytic root colonization exhibited a certain degree of host specificity as documented by rapid penetration of SA187 into wheat, barley and *Indigofera* roots, but slow or absent in the case of *Arabidopsis*, alfalfa and tomato roots. These observations might be due to variable compatibility of the enzymatic arsenal of SA187 with the distinct plant cell wall composition and possibly due to a specific pattern of root exudation in different plant species or taxonomic groups (Popper, 2008). In agreement, monocot species were endophytically colonized by *Klebsiella pneumoniae* to much higher levels than dicot species (Dong *et al.*, 2003), supporting the notion that endophytic colonization is controlled by both partners, PGPR and plant hosts, and these relations evolved during their co-evolution (Drogue *et al.*, 2012).

Soil bacteria often colonize not only roots, but also shoots as documented by approximately 50% overlap among bacterial species isolated from the rhizosphere and phyllosphere (Bai *et al.*, 2015). Although plants can close stomata to inhibit the entry of bacteria into their aerial parts, some pathogens produce coronatine or similar phytotoxins to induce stomatal re-opening (McLachlan *et al.*, 2014). Since SA187 lacks genes encoding the conventional coronatine biosynthesis, this strain likely produces another compound with a similar role or synthesizes coronatine using an alternative pathway. We suggest that PGPR have developed specialized mechanisms, resembling those of pathogenic bacteria, to overcome stomatal immunity.

Plant trichomes represent common infection sites in leaves for fungal and bacterial endophytes (Schneider and Grogan, 1977; Barak *et al.*, 2011; Chalupowicz *et al.*, 2017; Kim, 2019). The short oval secretory trichomes that we found colonized by SA187 in the native host are common to many *Indigofera* species (Marquiafével *et al.*, 2009). Whereas hairy trichomes provide physical protection against herbivores, glandular (incl. secretory) trichomes have been associated with defence mechanisms and inter-species communication – both functions residing in the production of various volatiles (Glas *et al.*, 2012). Indole and other volatiles are known to either induce defence genes or have antimicrobial activities by themselves (De Vrieze *et al.*, 2015; Erb *et al.*, 2015; Lee *et al.*, 2015; Méndez-Bravo *et al.*, 2018;

Agisha *et al.*, 2019; Eida *et al.*, 2020). Because SA187 can produce a significant amount of indole and the production of volatiles seems to be common to PGPR (Blom *et al.*, 2011), it is tempting to speculate that these compounds, which have been so far attributed to be emitted by plant secretory trichomes, might actually be derived from trichome-hosted microbes. In this case, PGPR would benefit from a source of nutrients and a convenient micro-environment in secretory trichomes. The association of secretory trichomes with microbes has been rarely studied so far (Karamanoli *et al.*, 2012), but warrants further investigations as a novel element of plant–microbe interactions.

In conclusion, we presented detailed microscopic characterization of Arabidopsis colonization by beneficial *Enterobacter* sp. SA187 that may serve as a blueprint for comprehensive documentation of plant colonization processes by a PGPR. Novel observations, such as the preferential association of SA187 with the micropylar pole in pre-germinating seeds or the lower colonization of lateral roots in contrast to primary roots will require further studies. Finally, the efficient epiphytic and endophytic colonization of crops, such as wheat and barley seedlings, highlights the potential use of SA187 in agriculture.

Experimental procedures

Bacterial and plant material

Enterobacter sp. SA187 isolated from roots of *I. argentea* was characterized in Andres-Barrao *et al.* (2017). Generation of GFP-tagged SA187 was described in de Zélicourt *et al.* (2018). *Pseudomonas syringae* pv. *tomato* DC3000 was used in the stomatal opening assay. Bacterial strains *Microbacterium oryzae* JZ102 (KY194299) and *Bacillus safensis* JZ33 (KY194242) were from the microbial collection in KAUST (Saudi Arabia).

Plant material included *I. argentea* (collected in Jizan, Saudi Arabia), *A. thaliana* Col-0 (SALK collection), wheat (*Triticum aestivum* variety Yecora Rojo), barley (*Hordeum vulgare* variety Qassimi), alfalfa (*Medicago sativa* variety CUF 101) and tomato (*Solanum lycopersicum* variety Ginan).

Plant inoculation and growth conditions

For colonization experiments *in vitro*, seeds of *Arabidopsis*, *Indigofera*, alfalfa, tomato, wheat or barley were surface sterilized on shaker for 10 min in 70% ethanol with 0.05% SDS, washed with 96% ethanol and let to dry. Arabidopsis seeds were stratified at 4°C for 3 days. Seeds were then plated on SA187-inoculated vertical MS agar plates [1/2× Murashige and Skoog basal salts (Sigma), 1% Agar A-1296 (Sigma), pH 5.7]. No sugar

was used in the medium. Inoculation procedure: overnight culture of SA187 from LB medium was washed with water and added at final concentration of 2×10^5 cells per ml to the autoclaved and pre-cooled MS medium (de Zélicourt *et al.*, 2018).

For observation of root endophytic colonization and shoot colonization, a strip of agar was removed from the top part of agar plates and seeds were put on the edge of agar to avoid direct contact of mature cotyledons with the inoculated agar medium.

For colonization experiments in soil, sandy soil collected at slopes of mountains north of Jeddah was used. Suspension of SA187 (2×10^6 cells per ml) prepared from an overnight culture in LB medium was sprayed over the soil surface (approximately 0.25 ml·cm⁻²). Seeds were then put directly onto the soil surface.

All plants were cultivated under long day conditions (16 h light/8 h dark) at 22°C in growth chambers (Percival). *Indigofera* was grown at 28°C.

Sample preparation and imaging

Colonized seedlings grown on MS agar plates or in soil were gently washed in liquid MS medium and aligned on a sterile MS plate. For imaging of seed colonization, translucent layer and cell motility, this washing was skipped. A block of agar with seedlings was cut out and placed upside-down to a Lab-Tek chamber with a drop of liquid MS medium as mounting medium. PI was added at 30 μM final concentration whenever visualization of plant cell walls or damaged/dead cells was needed (PI stains the plasma membrane of intact cells but also the cytoplasm and nucleus in impaired cells).

For analysis of bacterial attraction to roots in liquid medium, 4-day-old sterile seedlings were mounted between slides with bacterial suspension (O.D.₆₀₀ = 0.005) in MS medium, incubated for 30 min, and time-lapse series were taken at 10s intervals for 5 min focused on the medial root plane. Each series was then corrected for drift using the Drift Correction plugin in FIJI, and MIP in time was rendered.

For observation of the seed colonization, translucent layer and strength of attachment, agar blocks with seedlings were placed upright on glass slides and observed without mounting.

Samples were imaged using inverted Zeiss LSM 880 or upright LSM 710 confocal microscopes equipped with Plan-Apochromat 10×/0.45, Plan-Apochromat 20×/0.8, and Plan-Apochromat 40×/1.3 Oil objectives. Wavelengths of excitation lasers and captured emission (in nm) were as follows: blue autofluorescence of seed coats, 405/411–483; GFP, 488/493–537; PI and red autofluorescence, 561/579–637 nm; far-red autofluorescence, 561/645–708. DIC contrast was applied to visualize root or trichome morphology.

Z-stacks were taken at 2 μm steps using 40 \times objective or 10 μm steps using 10 \times objective and then processed to render MIP or 3D reconstructions in ZEN Black (Zeiss).

Quantification of root colonization

Using the cultivation-based approach for bacterial quantification, we follow the protocol Saad *et al.* (2018). Shortly, roots segments approximately 1 cm long were separated by a scalpel (new/old parts for Fig. 4D; primary/lateral roots for Fig. 5B), collected, weighted, gently washed in distilled water to remove non-attached bacterial cells, and then processed. Harvested material was ground in micro-tubes using tissue grinder pestles (Fisher Scientific). After adding 1 ml of extraction buffer (10 mM MgCl_2 , 0.01% Silwet L-77), samples were sonicated three times for 5 s and subsequently vortexed for 10 min. Each sample was serially diluted in 10-fold scale and spread on LB agar plates in technical triplicates. Colony forming units (CFU) were counted after overnight incubation at 28°C and normalized to root fresh weight. Each sample consisted of five root segments. At least 12 samples were collected for each category in one experiment, and the experiment was conducted in three biological replicates.

Using the fluorescence-based approach (in Fig. 4F), 4-day-old colonized roots were imaged without mounting using 10 \times objective to obtain Z-stacks at 10 μm steps. Each seedling was washed after imaging and placed at the same orientation on a new block of agar and imaged again (holding seedlings by tweezers during washing ensured similar position of roots after manipulation). Only the top half of each root (i.e. excluding that half attached to agar) was imaged. MIP were generated from Z-stacks. Mean GFP fluorescence intensity was measured in every root zone; root borders were avoided. The meristematic zone was analysed as one region of interest, while elongation and differentiation zones as three neighbouring regions of interest. Seven roots were examined in each of three biological replicates.

Quantification of cell motility

For analysis of cell motility, 4-day-old seedlings were mounted into Lab-Tek chambers without washing roots. Time-lapse series of SA187-GFP fluorescence were taken using 40 \times objective at 2 s intervals for 3 min. Each series was corrected in FIJI for bleaching using the Bleach Correction plugin and for drift of growing roots using the Drift Correction plugin before calculating average projections and MIP. The averaged output was then used as Green channel of a new image, while the MIP output as Red and Blue channels, resulting in visualization of non-motile cells in white in merged images. Average cell motility in colonies across different root zones

was determined as a ratio of mean grey value in Red to Green channel in merged images. A group of more than five cells was considered as a colony. Six roots were imaged at five distinct positions from the meristematic to differentiation zone. The experiment was performed in three biological replicates.

Enzymatic assays

Bacterial suspension ($\text{O.D.}_{600} = 0.2$) prepared from overnight culture was dropped in six replicates onto agar plates containing pectin, cellulose or skim milk as the major carbon source. See Method S1 for media composition. Plates with bacteria were incubated at 28°C for 2 days (pectin, skim milk) or 14 days (cellulose). Presence of a clear zone was indicative of enzymatic digestion of the main substrate. To evaluate cellulose and pectin digestion, bacterial colonies were washed off from the agar surface. For pectin digestion, agar plates were then flooded with 1% cetyltrimethylammonium bromide (CTAB) for 3 h. The experiment was performed in three replicates.

Stomatal aperture assay

We followed a standard procedure described in Abulfaraj *et al.* (2018). At least 30 stomata were measured in each leaf segment, three segments were used for each condition, and the experiment was repeated in three biological replicates. Average values calculated for each leaf segment were again averaged for each condition providing the final mean value. Final mean values of treated samples were normalized to those of untreated samples.

Collection and identification of volatiles using gas chromatography–mass spectrometry

This analysis was performed according to De Vrieze *et al.* (2015). See Method S2 for technical details.

Statistical analysis

T-test and ANOVA statistical analyses were performed using the NCSS 12 software (www.ncss.com). Graphs were imported and formatted in Inkscape 1.0 (www.inkscape.org).

Acknowledgements

We thank to I. Blilou (KAUST) for critical reading of the manuscript. This work was supported by the KAUST project No. BAS/1/1062-01-01 to H.H. and by the Swiss National Science Foundation project No. 31003A_179310 to L.W. We thank to developers of FIJI and Inkscape software.

References

- Abulfaraj, A.A., Mariappan, K., Bigeard, J., Manickam, P., Bliou, I., Guo, X., et al. (2018) The Arabidopsis homolog of human G3BP1 is a key regulator of stomatal and apoplastic immunity. *Life Sci Alliance* **1**: e201800046.
- Agisha, V.N., Kumar, A., Eapen, S.J., Sheoran, N., and Suseelabhai, R. (2019) Broad-spectrum antimicrobial activity of volatile organic compounds from endophytic *Pseudomonas putida* BP25 against diverse plant pathogens. *Biocontrol Sci Technol* **29**: 1069–1089.
- Andres-Barrao, C., Lafi, F.F., Alam, I., de Zélicourt, A., Eida, A.A., Bokhari, A., et al. (2017) Complete genome sequence analysis of *Enterobacter* sp. SA187, a plant multi-stress tolerance promoting endophytic bacterium. *Front Microbiol* **8**: 1–21.
- Ankati, S., and Podile, A.R. (2019) Metabolites in the root exudates of groundnut change during interaction with plant growth promoting rhizobacteria in a strain-specific manner. *J Plant Physiol* **243**: 153057.
- Backer, R., Rokem, J.S., Ilangumaran, G., Lamont, J., Praslickova, D., Ricci, E., et al. (2018) Plant growth-promoting rhizobacteria: context, mechanisms of action, and roadmap to commercialization of biostimulants for sustainable agriculture. *Front Plant Sci* **9**: 1473.
- Bai, Y., Müller, D.B., Srinivas, G., Garrido-Oter, R., Potthoff, E., Rott, M., et al. (2015) Functional overlap of the Arabidopsis leaf and root microbiota. *Nature* **528**: 364–369.
- Bais, H.P., Weir, T.L., Perry, L.G., Gilroy, S., and Vivanco, J. M. (2006) The role of root exudates in rhizosphere interactions with plants and other organisms. *Annu Rev Plant Biol* **57**: 233e266.
- Balachandar, D., Sandhiya, G.S., Sugitha, T.C.K., and Kumar, K. (2006) Flavonoids and growth hormones influence endophytic colonization and in planta nitrogen fixation by a diazotrophic *Serratia* sp. in rice. *World J Microbiol Biotechnol* **22**: 707–712.
- Barak, J.D., Kramer, L.C., and Hao, L. (2011) Colonization of tomato plants by *Salmonella enterica* is cultivar dependent and type I glandular trichomes are preferred colonization sites. *Appl Environ Microbiol* **77**: 498–504.
- Berg, G., and Smalla, K. (2009) Plant species and soil type cooperatively shape the structure and function of microbial communities in the rhizosphere. *FEMS Microbiol Ecol* **68**: 1–13.
- Bisseling, T., Dangl, J.L., and Schulze-Lefert, P. (2009) Next-generation communication. *Science* **324**: 691.
- Blom, D., Fabbri, C., Connor, E.C., Schiestl, F.P., Klausner, D.R., Boller, T., et al. (2011) Production of plant growth modulating volatiles is widespread among rhizosphere bacteria and strongly depends on culture conditions. *Environ Microbiol* **13**: 3047–3058.
- Chalupowicz, L., Barash, I., Reuven, M., Dror, O., Sharabani, G., Gartemann, K.-H., et al. (2017) Differential contribution of *Clavibacter michiganensis* ssp. *michiganensis* virulence factors to systemic and local infection in tomato. *Mol Plant Pathol* **18**: 336–346.
- Cherif-Silini, H., Thissera, B., Bouket, A.C., Saadaoui, N., Silini, A., Eshelli, M., et al. (2019) Durum wheat stress tolerance induced by endophyte *Pantoea agglomerans* with genes contributing to plant functions and secondary metabolite arsenal. *Int J Mol Sci* **20**: 3989.
- Compant, S., Reiter, B., Nowak, J., Sessitsch, A., Clément, C., and Barka, E.A. (2005) Endophytic colonization of *Vitis vinifera* L. by plant growth-promoting bacterium *Burkholderia* sp. strain PsJN. *Appl Environ Microbiol* **71**: 1685–1693.
- De Giorgi, J., Piskurewicz, U., Loubery, S., Utz-Pugin, A., Bailly, C., Mène-Saffrané, L., and Lopez-Molina, L. (2015) An endosperm-associated cuticle is required for Arabidopsis seed viability, dormancy and early control of germination. *PLoS Genet* **11**: e1005708.
- De Vrieze, M., Pandey, P., Bucheli, T.D., Varadarajan, A.R., Ahrens, C.H., Weisskopf, L., and Bailly, A. (2015) Volatile organic compounds from native potato-associated *Pseudomonas* as potential anti-oomycete agents. *Front Microbiol* **6**: 1295.
- Dietel, K., Beator, B., Budiharjo, A., Fan, B., and Borriss, R. (2013) Bacterial traits involved in colonization of *Arabidopsis thaliana* roots by *Bacillus amyloliquefaciens* FZB42. *Plant Pathol J* **29**: 59–66.
- Dong, Y., Iniguez, A.L., and Triplett, E.W. (2003) Quantitative assessments of the host range and strain specificity of endophytic colonization by *Klebsiella pneumoniae* 342. *Plant and Soil* **257**: 49–59.
- Drogue, B., Doré, H., Borland, S., Wisniewski-Dyé, F., and Prigent-Combaret, C. (2012) Which specificity in cooperation between phyto-stimulating rhizobacteria and plants? *Res Microbiol* **163**: 500–510.
- Eida, A.A., Alzubaidy, H.S., de Zélicourt, A., Synek, L., Alsharif, W., Lafi, F.F., et al. (2019) Phylogenetically diverse endophytic bacteria from desert plants induce transcriptional changes of tissue-specific ion transporters and salinity stress in *Arabidopsis thaliana*. *Plant Sci* **280**: 228–240.
- Eida, A.A., Bougouffa, S., L'Haridon, F., Alam, I., Weisskopf, L., Bajic, V.B., et al. (2020) Genome insights of the plant-growth promoting bacterium *Cronobacter mytjensii* JZ38 with volatile-mediated antagonistic activity against *Phytophthora infestans*. *Front Microbiol* **11**: 369.
- Erb, M., Veyrat, N., Robert, C.A., Xu, H., Frey, M., Ton, J., and Turlings, T.C. (2015) Indole is an essential herbivore-induced volatile priming signal in maize. *Nat Commun* **6**: 6273.
- Fendrych, M., Synek, L., Pecenkova, T., Drdova, E.J., Sekeres, J., de Rycke, R., et al. (2013) Visualization of the exocyst complex dynamics at the plasma membrane of *Arabidopsis thaliana*. *Mol Biol Cell* **24**: 510–520.
- Frank, A.C., Saldierna Guzmán, J.P., and Shay, J.E. (2017) Transmission of bacterial endophytes. *Microorganisms* **5**: 70.
- Fukaki, H., Tameda, S., Masuda, H., and Tasaka, M. (2002) Lateral root formation is blocked by a gain-of-function mutation in the SOLITARY-ROOT/IAA14 gene of Arabidopsis. *Plant J* **29**: 153–168.
- Gamalero, E., Lingua, G., Capri, F.G., Fusconi, A., Berta, G., and Lemanceau, P. (2004) Colonization pattern of primary tomato roots by *Pseudomonas fluorescens* A6RI characterized by dilution plating, flow cytometry, fluorescence, confocal and scanning electron microscopy. *FEMS Microbiol Ecol* **48**: 79–87.
- Glas, J.J., Schimmel, B.C., Alba, J.M., Escobar-Bravo, R., Schuurink, R.C., and Kant, M.R. (2012) Plant glandular tri-

- chomes as targets for breeding or engineering of resistance to herbivores. *Int J Mol Sci* **13**: 17077–17103.
- Grayston, S.J., Vaughan, D., and Jones, D. (1996) Rhizosphere carbon flow in trees, in comparison with annual plants: the importance of root exudation and its impact on microbial activity and nutrient availability. *Appl Soil Ecol* **5**: 29–56.
- Haichar, F.Z., Marol, C., Berge, O., Rangel-Castro, J.I., Prosser, J.I., Balesdent, J., *et al.* (2008) Plant host habitat and root exudates shape soil bacterial community structure. *ISME J* **2**: 1221–1230.
- Haichar, F.Z., Santaella, C., Heulin, T., and Achouak, W. (2014) Root exudates mediated interactions belowground. *Soil Biol Biochem* **77**: 69–80.
- Hansen, M.L., Kregelund, L., Nybroe, O., and Sørensen, J. (1997) Early colonization of barley roots by *Pseudomonas fluorescens* studied by immunofluorescence technique and confocal laser scanning microscopy. *FEMS Microbiol Ecol* **23**: 353e360.
- Hardoim, P.R., van Overbeek, L.S., Berg, G., Pirttilä, A.M., Compant, S., Campisano, A., *et al.* (2015) The hidden world within plants: ecological and evolutionary considerations for defining functioning of microbial endophytes. *Microbiol Mol Biol Rev* **79**: 293–320.
- Haughn, G.W., and Western, T.L. (2012) Arabidopsis seed coat mucilage is a specialized cell wall that can be used as a model for genetic analysis of plant cell wall structure and function. *Front Plant Sci* **3**: 64.
- Hirt, H. (2020) Healthy soils for healthy plants for healthy humans: how beneficial microbes in the soil, food and gut are interconnected and how agriculture can contribute to human health. *EMBO Rep* **21**: e51069.
- Humphris, S.N., Bengough, A.G., Griffiths, B.S., Kilham, K., Rodger, S., Stubbs, V., *et al.* (2005) Root cap influences root colonisation by *Pseudomonas fluorescens* SBW25 on maize. *FEMS Microbiol Ecol* **54**: 123–130.
- Hurek, T., Reinhold-Hurek, B., Van Montagu, M., and Kellenberger, E. (1994) Root colonization and systemic spreading of *Azoarcus* sp. strain BH72 in grasses. *J Bacteriol* **176**: 1913–1923.
- Karamanoli, K., Thalassinou, G., Karpouzias, D., Bosabalidis, A.M., Vokou, D., and Constantinidou, H.-I. (2012) Are leaf glandular trichomes of oregano hospitable habitats for bacterial growth? *J Chem Ecol* **38**: 476–485.
- Kawamura-Sato, K., Shibayama, K., Horii, T., Iimura, Y., Arakawa, Y., and Ohta, M. (1999) Role of multiple efflux pumps in *Escherichia coli* in indole expulsion. *FEMS Microbiol Lett* **179**: 345–352.
- Kim, K.W. (2019) Plant trichomes as microbial habitats and infection sites. *Eur J Plant Pathol* **154**: 157–169.
- Langowski, L., Ruzicka, K., Naramoto, S., Kleine-Vehn, J., and Friml, J. (2010) Trafficking to the outer polar domain defines the root-soil interface. *Curr Biol* **20**: 904–908.
- Lee, J.H., Wood, T.K., and Lee, J. (2015) Roles of indole as an interspecies and interkingdom signaling molecule. *Trends Microbiol* **23**: 707–718.
- Li, G., and Young, K.D. (2013) Indole production by the tryptophanase TnaA in *Escherichia coli* is determined by the amount of exogenous tryptophan. *Microbiology* **159**: 402–410.
- Liu, H., Carvalhais, L.C., Crawford, M., Singh, E., Dennis, P.G., Pieterse, C.M.J., and Schenk, P.M. (2017) Inner plant values: diversity, colonization and benefits from endophytic bacteria. *Front Microbiol* **8**: 2552.
- Marasco, R., Rolli, E., Ettoumi, B., Vigani, G., Mapelli, F., Borin, S., *et al.* (2012) A drought resistance-promoting microbiome is selected by root system under desert farming. *PLoS One* **7**: e48479.
- Marquiasável, F.S., Ferreira, M.D., and de Pádua Teixeira, S. (2009) Novel reports of glands in Neotropical species of *Indigofera* L. (Leguminosae, Papilionoideae). *Flora* **204**: 189–197.
- Massalha, H., Korenblum, E., Malitsky, S., Shapiro, O.H., and Aharoni, A. (2017a) Live imaging of root-bacteria interactions in a microfluidics setup. *Proc Natl Acad Sci USA* **114**: 4549–4554.
- Massalha, H., Korenblum, E., Tholl, D., and Aharoni, A. (2017b) Small molecules below-ground: the role of specialized metabolites in the rhizosphere. *Plant J* **90**: 788–807.
- Mclachlan, D.H., Kopischke, M., and Robatzek, S. (2014) Gate control: guard cell regulation by microbial stress. *New Phytol* **203**: 1049–1063.
- Melotto, M., Underwood, W., Koczan, J., Nomura, K., and He, S.Y. (2006) Plant stomata function in innate immunity against bacterial invasion. *Cell* **126**: 969–980.
- Méndez-Bravo, A., Cortazar-Murillo, E.M., Guevara-Avenidaño, E., Ceballos-Luna, O., Rodríguez-Haas, B., Kiel-Martínez, A.L., *et al.* (2018) Plant growth-promoting rhizobacteria associated with avocado display antagonistic activity against *Phytophthora cinnamomi* through volatile emissions. *PLoS One* **13**: e0194665.
- Morley-Smith, E.R., Pike, M.J., Findlay, K., Kockenberger, W., Hill, L.M., Smith, A.M., and Rawsthorne, S. (2008) The transport of sugars to developing embryos is not via the bulk endosperm in oilseed rape seeds. *Plant Physiol* **147**: 2121–2130.
- Mukherjee, P., Mitra, A., and Roy, M. (2019) Halomonas rhizobacteria of *Avicennia marina* of Indian Sundarbans promote rice growth under saline and heavy metal stresses through exopolysaccharide production. *Front Microbiol* **10**: 1207.
- Peng, J., Li, Z., Wen, X., Li, W., Shi, H., Yang, L., *et al.* (2014) Salt-induced stabilization of EIN3/EIL1 confers salinity tolerance by deterring ROS accumulation in Arabidopsis. *PLoS Genet* **10**: e1004664.
- Popper, Z. (2008) Evolution and diversity of green plant cell walls. *Curr Opin Plant Biol* **11**: 286–292.
- Quadt-Hallmann, A., Kloepper, J.W., and Benhamou, N. (1997) Bacterial endophytes in cotton: mechanisms of entering the plant. *Can J Microbiol* **43**: 577–582.
- Reinhold-Hurek, B., Maes, T., Gemmer, S., Van Montagu, M., and Hurek, T. (2006) An endoglucanase is involved in infection of rice roots by the not-cellulose-metabolizing endophyte *Azoarcus* sp. strain BH72. *Mol Plant Microbe Interact* **19**: 181–188.
- Reinhold-Hurek, B., Bünger, W., Burbano, C.S., Sabale, M., and Hurek, T. (2015) Roots shaping their microbiome: global hotspots for microbial activity. *Annu Rev Phytopathol* **53**: 403–424.
- Rudrappa, T., Czymmek, K.J., Paré, P.W., and Bais, H.P. (2008) Root-secreted malic acid recruits beneficial soil bacteria. *Plant Physiol* **148**: 1547–1556.

- Saad, M., de Zélicourt, A., Rolli, E., Synek, L., and Hirt, H. (2018) Quantification of root colonizing bacteria. *Bio-protocol* **8**: e2927.
- Saad, M.M., Eida, A.A., and Hirt, H. (2020) Tailoring plant-associated microbial inoculants in agriculture – a roadmap for successful application. *J Exp Bot* **71**: 3878–3901.
- Schneider, R.W., and Grogan, R.G. (1977) Tomato leaf trichomes, a habitat for resident populations of *Pseudomonas tomato*. *Phytopathology* **67**: 898–902.
- Sessitsch, A., Hardoim, P., Döring, J., Weilharter, A., Krause, A., Woyke, T., et al. (2012) Functional characteristics of an endophyte community colonizing rice roots as revealed by metagenomic analysis. *Mol Plant Microbe Interact* **25**: 28–36.
- Shekhawat, K., Saad, M.M., Sheikh, A., Mariappan, K., Al-Mahmoudi, H., Abdulhakim, F., et al. (2021) Root endophyte induced plant thermotolerance by constitutive chromatin modification at heat stress memory gene loci. *EMBO Rep* **22**: e51049.
- Stoeckle, D., Thellmann, M., and Vermeer, J.E. (2018) Breakout-lateral root emergence in *Arabidopsis thaliana*. *Curr Opin Plant Biol* **41**: 67–72.
- Tiwari, S., Prasad, V., Chauhan, P.S., and Lata, C. (2017) *Bacillus amyloliquefaciens* confers tolerance to various abiotic stresses and modulates plant response to phytohormones through osmoprotection and gene expression regulation in rice. *Front Plant Sci* **8**: 1510.
- Wang, W., Vinocur, B., and Altman, A. (2003) Plant responses to drought, salinity and extreme temperatures: towards genetic engineering for stress tolerance. *Planta* **218**: 1–14.
- Webster, G., Jain, V., Davey, M.R., Gough, C., Vasse, J., Denarie, J., and Cocking, E.C. (1998) The flavonoid naringenin stimulates the intercellular colonization of wheat roots by *Azorhizobium caulinodans*. *Plant Cell Environ* **21**: 373–383.
- Wheatley, R., and Poole, P. (2018) Mechanisms of bacterial attachment to roots. *FEMS Microbiol Rev* **42**: 448–461.
- Yuan, J., Zhao, J., Wen, T., Zhao, M., Li, R., Goossens, P., et al. (2018) Root exudates drive the soil-borne legacy of aboveground pathogen infection. *Microbiome* **6**: 156.
- Zamil, M.S., and Geitmann, A. (2017) The middle lamella more than a glue. *Phys Biol* **14**: 015004.
- Zamioudis, C., Mastranesti, P., Dhonukshe, P., Blilou, I., and Pieterse, C.M. (2013) Unraveling root developmental programs initiated by beneficial *Pseudomonas* spp. bacteria. *Plant Physiol* **162**: 304–318.
- de Zélicourt, A., Al-Yousif, M., and Hirt, H. (2013) Rhizosphere microbes as essential partners for plant stress tolerance. *Mol Plant* **6**: 242–245.
- de Zélicourt, A., Synek, L., Saad, M.M., Alzubaidy, H., Jalal, R., Xie, Y., et al. (2018) Ethylene induced plant stress tolerance by *Enterobacter* sp. SA187 is mediated by 2-keto-4-methylthiobutyric acid production. *PLoS Genet* **14**: e1007273.

Supporting Information

Additional Supporting Information may be found in the online version of this article at the publisher's web-site:

Table S1. Main volatile compounds emitted by SA187.

Table S2. List of genes encoding putative pectinases in the SA187 genome.

Fig. S1. Representative chromatogram obtained with SA187 in comparison to the empty medium.

Fig. S2. Colonization of *Arabidopsis* seed coats.

Fig. S3. SA187 colonization generates a translucent layer around *Arabidopsis* roots *in vitro*.

Fig. S4. Experimental setup for the analysis of colonization dependence on an intact shoot-root system.

Fig. S5. Endophytic colonization of wild-type and *slr-1* roots by GFP-tagged SA187.

Fig. S6. SA187 entry through stomata in *Arabidopsis* cotyledons.

Method S1. Composition of media for enzymatic assays.

Method S2. Collection and identification of volatiles using gas chromatography–mass spectrometry.